Optimization of electric vehicle charge scheduling with consideration of battery degradation

Raka Jovanovic and Sertac Bayhan
Hamad bin Khalifa University
Doha, Qatar
Email:{rjovanovic,sbayhan}@hbku.edu.qa,

Islam Safak Bayram
University of Strathclyde
Glasgow, United Kingdom
Email: safak.bayram@strath.ac.uk

Keywords

≪Charge scheduling≫, ≪Optimization algorithm≫, ≪Vehicle-to-Grid≫

Abstract

In this work, we explore the potential of exploiting the demand-flexibility of electric vehicles (EVs) for flattening the electricity duck curve that emerge as a result of growing solar power production. The focus is on vehicle-to-grid technology in which smart charging allows bidirectional energy flow between EVs and the utility grid. The main objective of this study is to evaluate the impact of V2G technologies on battery degradation. To do that a mathematical model is developed in the form of a mixed integer linear program (MILP). In the MILP the battery degradation is modeled based on charge/discharge cycles using the rising edge method for which appropriate constraints are provided. The proposed method is used to asses the relation between battery degradation and the level of flattening of the duck curve that can be achieved in V2G systems at park and ride facilities. The conducted computational experiments, based on real world data, show that the additional degradation caused by battery discharge in such systems can be substantial and can reach close to 9% of battery degradation in standard V2G systems.

1 Introduction

In recent years, there has been an astonishing increase in the use of solar energy for electricity production. The main reasons for this growth are the need for lowering carbon emissions and improvements to air quality. This growth creates operational issues for the power grid operators. The main cause for this is the imbalance between peak electricity demand and renewable energy production during afternoons and mornings resulting in the "duck curve" issue. This results in the need for power system operators to ramp-up or ramp-down their production capacity, which leads to financial losses [1, 2]. With the further increase of solar electricity generation it is expected that the "duck curve" issue will grow further.

At the same time, many governments have incentivised the use of electric vehicles (EV) to meet net-zero emission goals. This has resulted in a fast growth of EVs adoption, and it is expected that in the near decades, EVs will become a primary mode of ground transportation. The demand flexibility of EV charging has a high potential to alleviate the "duck curve" related issues. To be more precise, the use of smart charging of large groups of vehicles can minimizes the ramp-up or ramp-down requirements of non-renewable power generation. Such use of EV charging, in combination with residential and industrial demand response programs, as well as energy storage technologies can significantly decrease the costs of power grid operators related to integration of renewable generation [3].

The majority of EV charging is done by one of three types of chargers. Firstly, by fast, Level 3 (50+ kW) chargers, that can fill a typical EV battery in less than 30 minutes. Level 1 (2-3 kW or up to 16 amps) chargers are generally used at residential premises and not well suited for demand side management due to low charge rates and the fact they are generally used for overnight charging when no electricity is

generated from solar power. In case of Level 3 chargers, the charging time is short and it is not practical for shifting demand. On the other hand, smart charging of such systems generally lowers the charging power, and decreases the main benefit of fast charging.

The most suitable type of chargers for smoothing "duck curves" are Level 2 ones (5-7 kW) since they are mostly used at parking lots (e.g. workplace, university, etc.) where EVs are parked for several hours [4, 5]. In recent years, extensive research has been conducted on optimizing the scheduling of EV charging with Level 2 chargers at parking lots [6–8]. The positive aspects of EV smart charging have been analyzed in the context of workplace parking [9–12], commercial [13] parking lots and park-and-ride (PR) facilities [14, 15]. The majority of this research is dedicated to systems that only allow EVs to receive power, commonly called grid-to-vehicle systems (G2V). Recently, more research effort has been dedicated to the evaluation of systems in which EVs can also provide energy from their batteries to the grid, known as vehicle-to-grid systems (V2G) [16, 17]. When analyzing such systems, it is necessary to consider battery degradation, since a significant part of an EV value is related to its battery. The problem is that modeling battery degradation is in essence nonlinear and results in complex optimization problems which are frequently solved using different types of gradient based [18, 19], heuristic [20] and metaheuristic [21] methods.

On the other hand, the use of linear or quadratic mixed-integer programs for modeling such systems can provide significant benefits. In [22] a mixed integer linear program (MILP) is developed to analyze financial costs of battery degradation in V2G systems, that is solved using iterative solution method. This paper focuses on defining a MILP for optimizing V2G systems with consideration of battery degradation that can be solved using standard solvers. To be more precise, the fact that battery degradation is related to charge/discharge cycles is a convex function is exploited to create a mixed integer linear program (MILP) for the problem of interest using piece-wise linear approximation. The developed mathematical model is used to evaluate the relation between battery degradation and the smoothing of the "duck curve". To be exact, this analysis is conducted based on real world data for PR facilities through a case study.

The paper is organized as follows. The following section provides an outline of the system being optimized and the corresponding mathematical model. Section 3 is dedicated to the MILP for the problem of interest. The next section focuses on the conducted experiments and their analyses. The paper is finalized with concluding remarks that are presented in the last section.

2 Mathematical model

In this section, the mathematical model for optimizing smart scheduling of EV charging with the goal of minimizing the "duck curve" is presented. The model considers a V2G system where multiple vehicles visit a charging facility using Level 2 chargers. The model analyses a setting in which bidirectional charging is allowed and it is possible for EVs to inject power back to the electrical grid from their batteries. This type of smart scheduling is also observed from the aspect of battery degradation induced by the use of EV batteries to provide energy to the grid. The objective of the model is to find an optimal charging schedule for all the EVs that are present in the station at the same time. To be more precise, the goal is to find the amount of power each EV receives or discharges at each time period.

In the following section, an outline of the model is provided along with the process to transform the problem into a MILP. Note that the practical problem of smart scheduling of EVs is an online one, in the sense that the information (EV charge levels etc.) is not initially available. The goal of this work is to evaluate the upper bounds of the benefits such systems can provide, because of this it is assumed that all the information is available to the optimization algorithm. In that sense, we follow the approach, based on neural networks proposed in [15], shows how optimal solutions acquired using a mixed integer program for smart EV scheduling can be used for finding near optimal solutions in an online setting.

2 Scheduling setup

The proposed model starts from the following assumptions. The scheduling is performed over a time window $\mathcal{T}$ which is divided into a set of periods $\{1,\dots,T\}$. Each time period $t \in \mathcal{T}$ has a parameter

q_t equal to the base electricity consumption minus the solar generation. Due to technological limits, all chargers in the system have the same maximal charging power c^{max} (in kW). This value provides information on how much power an EV can receive in one time periods. In addition, parameter d^{max} indicates the maximal power an EV can provide to the grid in one time period. It is assumed that a number of EVs $i \in \mathcal{E}$, $E = \{1,\ldots,M\}$ visit the charging station and that for each EV i the arrival time a_i and departure time l_i are known in advance. For each EV i, its battery capacity f_i and state of charge at arrival $0 \leq b_i^a \leq f_i$ are known. It is assumed that an EV is connected to a charger during the time it is at the station and can receive/discharge power during its stay. A battery of an EV can only be charged until its full capacity or discharged to a minimal allowed state of charge (SoC). It is assumed that the maximal charging power of the system is equal to the total charging potential of all the chargers in the station. Each EV i requests a certain amount of charge r_i, and the charging station must provide it with at least αr_i power during its visit to the station, where α is a predetermined constant. The flattening of the "duck curve" is done by minimizing the change in total load (sum of q_t and energy used for charging all the EVs) in successive time periods. A more detailed description of the objective function is provided in the next section that is dedicated to the MILP.

2 Battery degradation

There are several sources of EV battery degradation related to charging. Some major ones include battery temperature, charge/discharge cycles, and extreme states of charge, as reported in [22]. Battery temperature is generally related to weather and the use of fast chargers, and does not have a major impact in case of Level 2 chargers. Therefore, the focus is on charge/discharge cycles, since they are directly related to the use of EV batteries by the station operator for providing power to the grid. There are several approaches for cycle counting, the most commonly used methods are based on half-cycle, rising edge, rain flow, and max-edge analysis [23]. Aforementioned methods analyze the peaks of the corresponding load curve (or stress curve). A graphical illustration of these methods can be seen in Fig 1. The rainflow method is the most effective as it manages to track the amplitudes of short and long period cycles. The issue with this approach is that it does not have a closed form expression and, to the best of the authors' knowledge, does not a have a formulation suitable for linear programming. Because of this, models for battery degradation that use the rainflow method for cycle counting are generally optimized using metaheuristics such as particle swarm optimization [21]. It should be noted that there are also approaches to model the charge/discharge cycle-based battery degradation cost as convex function [18]. Consequently, gradient based methods have been developed for the related optimization problems [18,19]. On the other hand, although other methods provide cycle counts that have a higher error than the

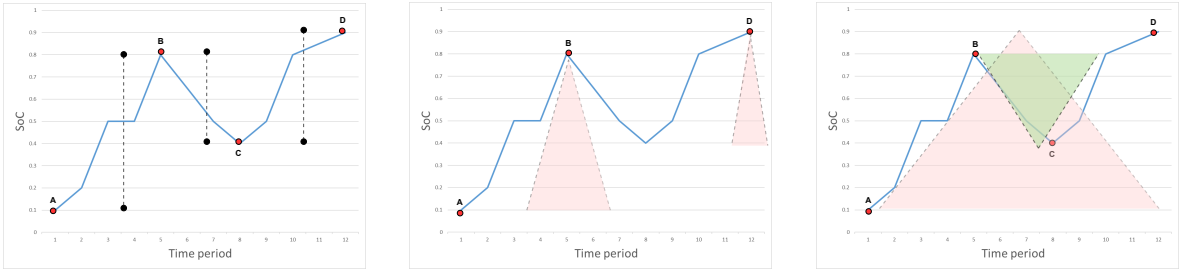

(a) Half cycle (b) Rising Edge (c) Rainflow

Fig. 1: Overview of different methods of cycle counting. Lines present half cycles and triangles full cycles. The amplitude of the cycles is given in the y axis.

rainflow method, they are commonly used since they can provide some insight in the problem of interest. Some comparison of the quality of cycle counts found by different methods can be found in [23]. In the proposed model, the selected approach for cycle counting is the rising edge method. The main reason is that the rising edge method can focus on the cycles that are induced by the battery discharges done by the charging station operator. Note that in this case, the method is applied to the load curve symmetric to the x-axis, so it could be called"falling edge" method. In a sense, it tracks the damage given to the

battery resulting from the use of an EV's battery by the charging station operator. In the next sections, it will be shown how rising edge based cycle counting can be included in a mixed integer linear program.

3 Mixed integer program

In this section, the details of the MILP for the proposed mathematical model are given. In practice, the MILP formulation is divided into the following components. The first one focuses on the charge/discharge power of EVs related to minimizing the duck curve. The second part of the model focuses on peak tracking and their use for evaluating battery degradation.

The model uses the following set of decision variables. For each EV $i \in \mathcal{E}$ and time period $t \in \mathcal{T}$ a real decision variables c_{it} is used to indicate the amount power an EV i receives at time period t. In the same way, decision variables d_{it}, defined for all $i \in \mathcal{E}$ and $t \in \mathcal{T}$, are used to indicate the amount of power that an EV i provides to the grid at time period t. Next, let us define real variables b_{it}, for all $i \in \mathcal{E}$ and $t \in \mathcal{T}$, equal to the SoC of EV i at time t. With the intention of having a simpler formulation, instead of parameters for arrival (a_i) and departure times (d_i) for an EV i, a set of binary parameters v_{it}, for all $i \in \mathcal{E}$ and $t \in \mathcal{T}$, are defined to indicate if EV i is at the charging station at time period t. The model

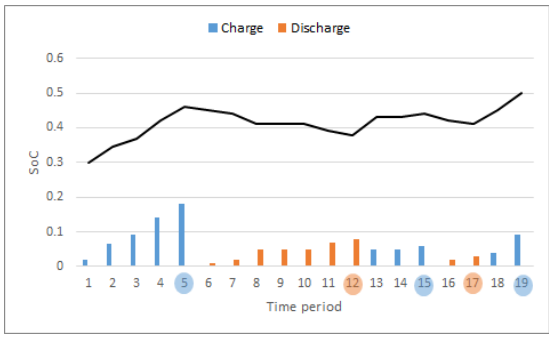

Fig. 2: Illustration of charge/discharge windows based on SoC. The color blue/orange is used for time period is in a charge/discharge window.

uses auxiliary real variables l_t, defined for all $t \in \mathcal{T}$, to store the information on the total load related to charging/discharging of the EVs currently at the station. Next, a set of auxiliary real variables C_t, defined for $t \in \mathcal{T}_0$ where $\mathcal{T}_0 = \mathcal{T} \setminus \{1\}$, is used the track the difference in total load (sum of base load and EV related load) between consecutive time periods.

Using these variables, the constraints for modeling an EV charging facility and the objective function for minimizing load ramp-up/ramp-down requirements can be specified. As in previously published research [12, 24], the minimization of ramp-up requirements is done based on the sum of the quadratic change in total load C_t overall the time periods. Due to the higher computational complexity of the proposed MIP, compared to the ones in [12,24], instead of using the sum of C_t^2 in the objective function, its linear piece-wise approximation is used, as

$$\text{Minimize} \sum_{t \in \mathcal{T}_0} lpa(C_t^2). \tag{1}$$

In Eq. (1), the notation $lpa(\cdot)$ is used for the linear piece-wise approximation of a function, which is a quadratic one. The next step in defining the proposed MILP, is specifying the constraints related to the SoC, charge and discharge powers for EVs and tracking the total load difference. The constraints are given in Eqs. (2)-(10) as shown below.

$$0 \leq d_{it} \leq d^{max} \qquad i \in \mathcal{E}, t_e \in \mathcal{T} \tag{2}$$
$$0 \leq c_{it} \leq c^{max} \qquad i \in \mathcal{E}, t_e \in \mathcal{T} \tag{3}$$
$$b_i^{min} \leq b_{it} \leq f_i \qquad i \in \mathcal{E}, t \in \mathcal{T} \tag{4}$$
$$\tag{5}$$

$$b_{i1} = b_i^a \qquad i \in \mathcal{E} \tag{6}$$
$$b_{it+1} = b_{it} + c_{it} - d_{it} \qquad i \in \mathcal{E}, t \in \mathcal{T}_0 \tag{7}$$
$$b_{tT} - b_i^a \geq \alpha r_i \qquad i \in \mathcal{E} \tag{8}$$
$$l_t = \sum_{i \in \mathcal{E}} (c_{it} - d_{it}) \qquad t \in \mathcal{T} \tag{9}$$
$$C_t = l_t + q_t - l_{t-1} - q_{t-1} \qquad t \in \mathcal{T}_0 \tag{10}$$

The Eqs. (2),(3) are used to specify the bounds on the amount of power an EV can receive or discharge at each time period. The constraints given in (4) guarantee that the SoC of each EV i at each time period t is bound by the battery capacity and minimal allowed state of charge. Next, the constraints given in Eqs. (6),(7) are used to guarantee that at each time period the b_{it} is equal to the correct SoC for EV i at time period t. The Eq. 8 guarantees that each EV receives at least the amount of charge promised by the charging station operator. The Eq. (9) is used to track the total load (l_t) related to EVs at the station at time period t. The Eq.(10) uses this value to get the changes in total load (C_t) between two consecutive time periods

It should be noted that two sets of non-negative decision variables for charging and discharging of EV batteries are used to make it possible to track peaks and valleys of the SoC curve for each EV. The idea for the constraints used to track peaks and valleys is to track continues charging or discharging windows. A discharging window consists of all time periods from the start of discharging until the first charging period (not included), see Fig. 2. Note that periods in which there is no charge or discharge will be considered being in the same window as the previous period. Now, peaks occur at time periods that are at the ends of charging windows and valleys occur at ends of discharging periods.

The following text describes the part of the MILP dedicated to the tracking of peaks and valleys of individual EVs SoC and how they are used for cycle counting. Firstly, let us define a auxiliary binary variables c_{it}^w and d_{it}^w, defined for $i \in \mathcal{E}$ and $t \in \mathcal{T}$, indicating if time period t for EV i is inside a charging or discharging window, respectively. Next, let us define a non-negative real variables d_{it}^s, defined for $i \in \mathcal{E}$ and $t \in \mathcal{T}$, providing the information on how much power has an EV discharged since the beginning of the current discharge window. The last set of auxiliary variables needed for peak tracking are d_{it}^p, which are equal to the d_{it}^s in case time period t corresponds to a peak and zero otherwise. The constraints specifying the behavior of the mentioned variables are given in Eqs. (11)-(28).

$$0 \leq c_{it}^w \leq 1, \qquad i \in \mathcal{E},\, t \in \mathcal{T} \tag{11}$$
$$0 \leq d_{it}^w \leq 1, \qquad i \in \mathcal{E},\, t \in \mathcal{T} \tag{12}$$
$$c_{it}^w + d_{it}^w = v_{it}, \qquad i \in \mathcal{E},\, t \in \mathcal{T} \tag{13}$$
$$c_{it} \leq M c_{it}^w, \qquad i \in \mathcal{E},\, t \in \mathcal{T} \tag{14}$$
$$d_{it} \leq M d_{it}^w, \qquad i \in \mathcal{E},\, t \in \mathcal{T} \tag{15}$$
$$c_{it+1}^w \geq c_{it}^w - d_{it}^w, \qquad i \in \mathcal{E}, t \in \mathcal{T} \tag{16}$$
$$d_{it+1}^w \geq d_{it}^w - c_{it}^w, \qquad i \in \mathcal{E},\, t \in \mathcal{T} \tag{17}$$
$$d_{i1}^s = d_{i1}, \qquad i \in \mathcal{E} \tag{18}$$
$$d_{it}^s \geq 0, \qquad i \in \mathcal{E},\, t \in \mathcal{T} \tag{19}$$
$$d_{it}^s \leq M(1 - c_{it}^a), \qquad i \in \mathcal{E},\, t \in \mathcal{T} \tag{20}$$
$$d_{it}^s \geq d_{it-1}^s + d_{it} - M c_{it}^a, \qquad i \in \mathcal{E},\, t \in \mathcal{T} \tag{21}$$
$$d_{it}^s \leq d_{it-1}^s + d_{it} + M c_{it}^a, \qquad i \in \mathcal{E},\, t \in \mathcal{T} \tag{22}$$
$$d_{it}^p \geq 0, \qquad i \in \mathcal{E},\, t \in \mathcal{T} \tag{23}$$
$$d_{it}^p \leq v_{it}, \qquad i \in \mathcal{E},\, t \in \mathcal{T} \tag{24}$$
$$d_{it}^p \leq d_{it}^s, \qquad i \in \mathcal{E},\, t \in \mathcal{T} \tag{25}$$

$$d^p_{it} \geq d^s_{it} - (1 - c^a_{it+1} + c^a_{it})M, \qquad i \in \mathcal{E},\, t \in \mathcal{T} \tag{26}$$
$$d^p_{it} \geq d^p_{min} - (1 - c^a_{it+1} + c^a_{it})M, \qquad i \in \mathcal{E},\, t \in \mathcal{T} \tag{27}$$
$$d^p_{it} \leq M c^a_{it+1}, \qquad i \in \mathcal{E},\, t \in \mathcal{T} \tag{28}$$

Eq. (13) states that for an EV i at time period t, is either in a charge or discharge window if it is at the charging station. Eqs. (14) and (15) guarantee that an EV can charge or discharge power only inside a charge or discharge window, respectively. In Eqs. (14) and (15), the notation M is used for a sufficiently large value in the standard way for large M constraints. The same notation is used later in the text. The constraints given in Eq. (16) guarantee that a charging window can only end with a discharge period. The Eq. (17) provides analogous constraints for discharge windows.

The next group of constraints is dedicated to the total amount of power that has been discharged during a discharge window. The constraints given in Eq. (18) are used to initialize the amount of discharge at the first time period. Eq. (20) states that in case of a charge period the total discharge is equal to 0. The constraints given in Eqs. (21),(22) are used for tracking the value of the total discharge in a discharge window between consecutive time periods. The Eqs. (21) and (22) state that the total amount of discharge in a discharge window, is equal to the total discharge in the previous time period increased by the current discharge.

The last group of constraints given in Eqs. (23)-(28) are related to recognizing the amount of total discharge at the end of a discharge window. The constraints given in Eq. (24) state that the total peak discharge is equal to 0, when an EV is not at the charging station. Eq. (25) states that the peak discharge at time period t is less than or equal to the total discharge in the discharge window at time period t. Constraints given in Eqs. (26) guarantees that the peak discharge is larger or equal to the total discharge at the end of a discharge window. The Eq. (27) guarantees that there is a minimal amount of discharge d^p_{min} that must happen in a discharge window. Although these constraints are not necessary to represent the real world systems, we have observed that there inclusion greatly decreases the computational cost of solving the MILP. The constraints given in (28) guarantee that a peak discharge at time period t can only be greater than 0 in case the following time period is in a charge window.

In the proposed MILP, as in [19], the battery degradation is modeled using the life loss from a single cycle of depth u measured in terms of (normalized) changes in the SoC. To be more precise, it is assumed that if a battery cell is repetitively cycled with depth u, then it can operate $\frac{1}{\Phi(u)}$ number of cycles before reaching its end of life. The degradation function $\Phi(u)$ is normalized between 0 and 1 with respect to the total battery life. In the proposed model the discharge cycle depth is calculated based on the peak discharge. As suggested in [19], the function $\Phi(u)$ is well approximated for electro-chemical batteries using the following formula

$$\Phi(u) = 0.524 \times 10^{-4} u^{2.03}. \tag{29}$$

Now, using the function $\Phi(u)$ the objective related to battery degradation can be included in the model in the following way

$$\text{Minimize} \sum_{i \in \mathcal{E}} \sum_{t \in \mathcal{T}} lpa(\Phi(d^p_{it})) \tag{30}$$

Eq. (30) uses the rising edge approach for analyzing battery discharge cycles using rising edges. Note that the rising edges correspond to the"decreasing edges" of an EV SOC. The total battery degradation is equal to the sum of degradation for all peak discharges for all EVs over all the time periods. Note that there is only one peak discharge for each window. It is important to point out that the proposed objective function, in practice, only considers the battery degradation induced by the discharge of batteries induced by the charging station operator. In the proposed model, due to computational complexity of the model instead of the function $\Phi(u)$ its piece-wise linear approximation $lpa(\Phi(u))$ is used.

4 Computational Experiments

In this section, the results of the conducted computational experiments are presented. The proposed MILP has been implemented using OPL in IBM ILOG CPLEX Optimization Studio Version: 12.6.1.0, and executed using the default solver settings. The computational experiments have been performed on a personal computer running Windows 10 having an Intel(R)Xeon(R) Gold 6244 CPU @3.60 GHz processor with 128 GB memory. The goal of the conducted computational experiments is to evaluate the potential of reducing the duck curve issue using a V2G system, in the sense of lowering ramping requirements in relation to battery degradation within an EV smart scheduling system. This is done based on real world data, with a special focus on park and ride (PR) facilities. In this section, firstly the method for incorporating such data in the model is presented. Next, details on the use of the proposed model are given and an analysis through a case study is provided.

4 Generation of data for experiments

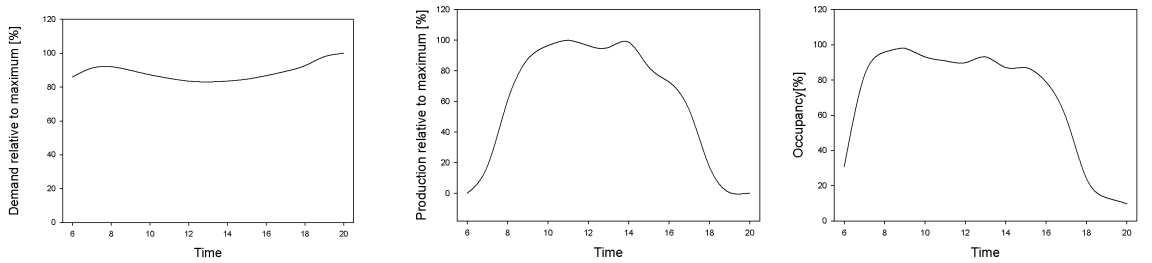

(a) Hourly total demand (b) Hourly solar generation (c) Hourly occupancy of park and ride facility

Fig. 3: Graphical illustration of data used for generating test instances taken from [25]. All the values are given in a normalized form and given in percentage.

The first group of parameters that need to be incorporated into the model are related to EV visits to the PR facilities. The data set that is used for this task is the hourly utilization rate of PR facilities taken from [25] (see Fig. 3(c) for a graphical illustration). This data is combined with metro passenger behavior statistics taken from [26]. The battery types of EVs have been randomly generated based on data related EV sales taken from [27] and corresponding battery sizes [28]. The SoC of individual batteries is randomly generated form the range 15% - 80% using a uniform distribution. This information is used to generate problem instances in the same way as in [14]. An extension of the proposed model, compared to [14], is the inclusion of requested amount of charge for EVs visiting the station. The requested charge is selected randomly, using a uniform distribution, 50% to 100% of battery capacity that can be maximally charged during the EVs stay at the facility.

The intention of the proposed model is to evaluate the relation of battery degradation and reductions in ramping requirements for varying percentages of solar generation and EV penetration levels. In the conducted case studies, the information on total demand and solar generation are taken from the publicly available data for California [29] and presented in Figs. 3(a) and 3(b). Using this data, separate problem instances have been generated for different portions of power used for EV charging and solar generation. To be more precise, it is assumed that the model optimizes the scheduling of N EVs and that the total requested power is E. Next, the base load and solar generation are scaled to be a specific proportion of this value. In other words, the normalized values given in Fig. 3 are multiplied by constants to get the correct proportion for EV consumption E, base load L and solar production S.

In generating the problem instances, the time period between 6:00 and 20:00 has been used to mimic actual operational times of PR parking lots. Each time period in the model corresponded to 15 minutes, which means the value of parameter T is 56. In the generated problem instances, a fixed number $N = 10$ is used for the number of EVs visiting the PR facility during the day. The potential of scheduling EV charging to minimize issues related to the "duck curve" are evaluated for settings where 15%, and 30% of

the maximal load is produced from solar generation. The assumed power of the chargers is 4 kW, which translates to $c_{max} = 1$ inside the model. The same value of maximal discharge power is used for $d_{max} = 1$. The chosen minimal amount of charge received by an EV was equivalent to 90% of the requested charge, hence $\alpha = 0.9$. The maximal amount of energy used for EV charging was 2.5% and 5.0% of the total energy consumption. The minimal total amount of discharge during a discharge window was 1.5 kWh.

4 Computational experiment setup

The objectives of the conducted research are to evaluate several aspects of the use of V2G systems. Firstly, to observe the level of decrease in ramping requirements of smart charge scheduling in V2G systems compared to G2V. Next, to evaluate the level of additional battery degradation that occurs in V2G compared to G2V systems. Finally, to see what is the maximal level of decrease in ramping requirements that can be achieved for different levels of battery degradation. To achieve this, the proposed model is used in the following way. A MILP using the objective function given in Eq. (1) is used to find the minimal value of the objective function $Ramp_{min}$ related to ramping requirements in V2G system. Note that this model only needs constraints given in Eqs. (2) - (10). The next step is finding the minimal level of battery degradation needed to achieve this level of decrease in ramping requirements. This is achieved, by minimizing the objective function given in Eq. (30) for the MILP given in constraints Eqs. (2)-(28) with the following additional constraint.

$$\sum_{t \in \mathcal{T}_0} lpa(C_t^2) \leq Ramp_{min} \tag{31}$$

In this way, the value of the objective function $DegBat_{min}$ related to minimal battery degradation for the maximal decrease in ramping requirements is acquired. The next step, is to evaluate the decrease in ramping requirements for different levels of battery degradation. Different levels, for $i \in \{0, ..., n\}$., of battery degradation $DegBat_i$ are specified using the following equation

$$DegBat_i = \frac{i}{n} DegBat_{min}. \tag{32}$$

For each value of $DegBat_i$ the maximal possible decrease in ramping requirements is calculated using a MILP with the objective function given in Eq. (1) with constraints given in Eqs. (2) - (28) with the addition of the following constraint.

$$\sum_{i \in \mathcal{E}} \sum_{t \in \mathcal{T}} lpa(\Phi(d_{it}^p)) \leq DegBat_i \tag{33}$$

Eq. (33) guarantees that the total battery degradation is less than $DegBat_i$. The used approach is equivalent to the standard ε-constraint method [30] for finding the Pareto Front of a bi-objective problem.

4 Case Study

The presented approach is used for a case study on the effect of smart charging in V2G systems at PR facilities. The method for incorporating real-world data has been provided in the previous section. The first set of results is given in Fig. 4 (left sub-figures), each of them provides information for settings with different levels of solar generation and EV adoption. Each of this figures shows the base load curve (base demand minus solar generation) over time. In addition, these figures contain load curves in which additional power is used for smart scheduling of EVs charging in G2V and V2G systems. In case of V2G two levels of battery degradation are considered. The first observation that can be drawn from these figures is that the V2G systems have a much higher impact on the load curve in the morning where there is a need for a high level of ramp-down (lowering of electricity production) than in the evening where there is need for ramp-up compared to G2V systems. One reason for this is that in the evening, there is a significant decrease of EVs at the PR facility due to drivers leaving after finishing their work day. The second reason is that at this period, it is necessary to have EVs that have received a higher amount of charge than requested that could potentially be discharged which is not possible for most of the EVs. Because of this, the focus of the quantitative analysis of V2G systems focuses on the morning period.

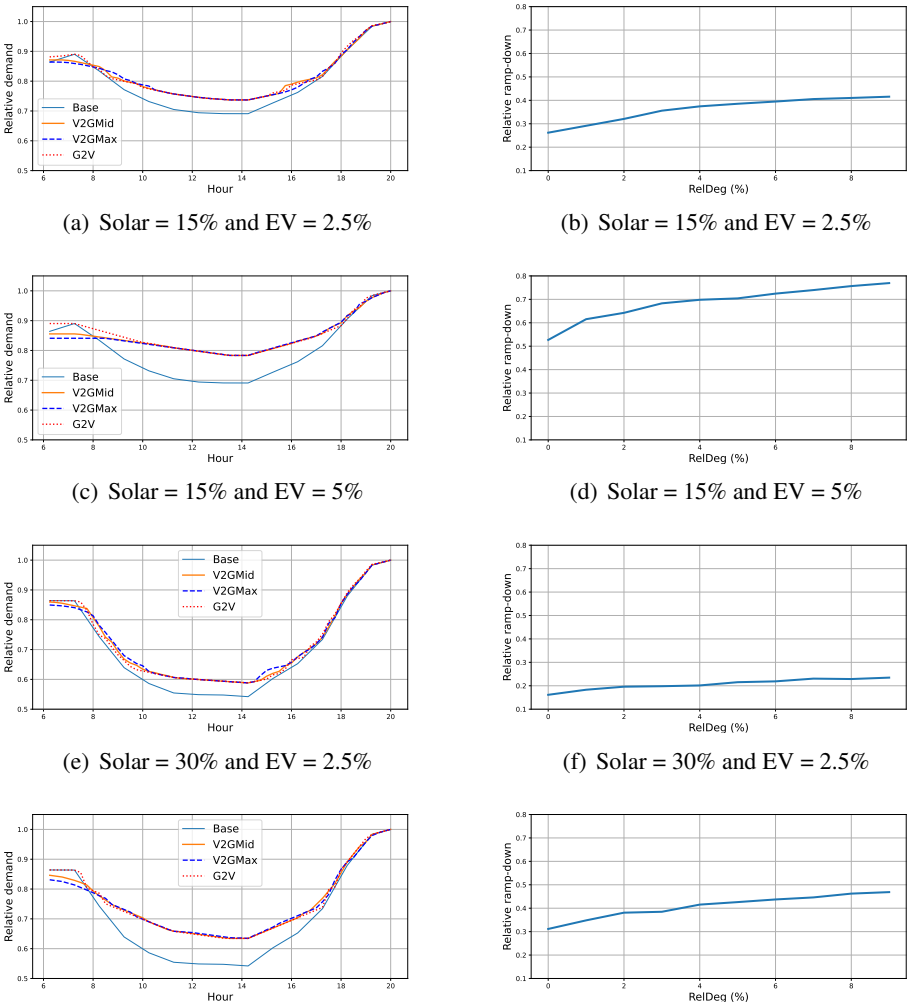

(a) Solar = 15% and EV = 2.5%

(b) Solar = 15% and EV = 2.5%

(c) Solar = 15% and EV = 5%

(d) Solar = 15% and EV = 5%

(e) Solar = 30% and EV = 2.5%

(f) Solar = 30% and EV = 2.5%

(g) Solar = 30% and EV = 5%

(h) Solar = 30% and EV = 5%

Fig. 4: Illustration of the effect of smart charging in V2G systems at PR facilities on the “duck curve”. Left side shows load curves for different levels of battery degradation. ”V2GMid” is used for battery degradation corresponding to the value $i = \frac{n}{2}$ in Eq.32. The right side shows the relation between relative battery degradation and relative ramp-down requirements. The values ”Solar” and ”EV” correspond to the percentage of the total energy consumption satisfied from solar or used by EVs.

The objective functions given in Eq. (1) and Eq. (30) are abstractions that are not suitable for understanding the relation of battery degradation and ramp-down requirements. Because of this the following measures are used to evaluate this relation. Firstly, the ramp-down requirements are observed using the difference between the maximal and minimal load in the time period between 7:15 and 11:30 divided by the time difference between them. The positive effect of the use of smart scheduling of EVs in G2V and V2G systems on ramp-down requirements is evaluated relative to the ramp-down requirements needed for the base load.

The battery degradation of V2G systems is analyzed in relation to the level of battery degradation in G2V systems. To be more precise, the additional battery degradation that occurs in V2G systems due to battery discharges relative to systems in which no discharge is allowed is observed. Formally, for each of the degradation level $DegBat_i$, the following equations are used to as a measure.

$$Deg_{Charge} = \sum_{e \in \mathcal{E}} \Phi\left(\frac{b_{iT} - b_i^a}{f_i}\right) \tag{34}$$

$$Deg_{Discharge} = \sum_{i \in \mathcal{E}} \sum_{t \in \mathcal{T}} \Phi(d_{it}^{p}) \tag{35}$$

$$RelDeg = \frac{Deg_{Discharge}}{Deg_{Charge}} \tag{36}$$

The Eq. (34) provide the battery degradation for all the EVs in the system based on the amount of charge each vehicle received. To be exact, for each EV i the amount of received charge equal to the SoC at arrival (b_i^a) minus the state of charge at departure (b_{iT}). The degradation is calculated using function Φ, so it is necessary to normalize the amount of received charge by the battery size. The battery degradation related to discharges is given in Eq. (35), and is the same as the objective function (33). Finally, the relative additional battery degradation is given in Eq. (36) as the total discharge degradation divided by the total charge related degradation.

The results on the relation of change in ramp-down requirements and battery degradation can be observed for different levels of EV adoption and solar generation in Fig. 4 (right sub-figures). Note that in these figures additional battery degradation of 0% corresponds to a G2V system. From these results, it is evident that the V2G systems provides a substantial additional decrease in ramp-down requirements. In case of solar generation of 15% G2V systems provide a decrease in ramp-down requirements of around 25% and 55% compared to 40% and 75% in case of V2G systems when EV charging consumes 2.5% and 5% of the total load, respectively. In case of solar generation of 30%, same values for G2V are 15% and 30% and grow to 25% and 45% in case of V2G, when EV charging consumes 2.5% and 5% of the total load, respectively. This maximal decrease in case of V2G system comes at a significant additional battery degradation which is close to 9% for all of the settings. It is important to point out that more than half of the decrease in ramp-down requirements can be achieved with an additional battery degradation of around 3% for the tested instances. These results indicate that although the use of smart charging in V2G systems for flattening the "duck curve" is effective it can result in significant additional cost for EV drivers. This negative effect can be substantially lowered if the optimization of the EV charge scheduling considers battery degradation.

5 Conclusion

In this paper, a mathematical model for analyzing the smart scheduling of EV charging in V2G system has been presented. The focus is on evaluating the relation of battery degradation and the potential for flattening of the "duck curve" in such systems. The proposed model is a MILP in which battery degradation is observed through charge/discharge cycles. It introduces a set of new constraints corresponding to the rising edge method which is highly suitable for evaluating battery degradation related to battery discharge induced by the charging station operator. The developed model is used to evaluate the potential of V2G systems at PR facilities based on real-world data. The conducted computational experiments indicate that, based on the new model, such systems are more suitable for lowering ramp-down requirements in the morning period than ramp-up requirements in the evening. It has been shown that smart scheduling of EV charging at such facilities can result in a substantial additional cost to EV drivers in case battery degradation is not considered.

References

[1] M. Obi and R. Bass, "Trends and challenges of grid-connected photovoltaic systems–a review," *Renewable and Sustainable Energy Reviews*, vol. 58, pp. 1082–1094, 2016.

[2] P. Denholm, M. O'Connell, G. Brinkman, and J. Jorgenson, "Overgeneration from solar energy in california. a field guide to the duck chart," National Renewable Energy Lab.(NREL), Golden, CO (United States), Tech. Rep., 2015.

[3] M. A. Zehir, A. Batman, and M. Bagriyanik, "Review and comparison of demand response options for more effective use of renewable energy at consumer level," *Renewable and Sustainable Energy Reviews*, vol. 56, pp. 631–642, 2016.

[4] D. Meyer and J. Wang, "Integrating ultra-fast charging stations within the power grids of smart cities: a review," *IET Smart Grid*, vol. 1, no. 1, pp. 3–10, 2018.

[5] I. Rahman, P. M. Vasant, B. S. M. Singh, M. Abdullah-Al-Wadud, and N. Adnan, "Review of recent trends in optimization techniques for plug-in hybrid, and electric vehicle charging infrastructures," *Renewable and Sustainable Energy Reviews*, vol. 58, pp. 1039–1047, 2016.
[6] X. Wu, "Role of workplace charging opportunities on adoption of plug-in electric vehicles–analysis based on gps-based longitudinal travel data," *Energy Policy*, vol. 114, pp. 367–379, 2018.
[7] B. Ferguson, V. Nagaraj, E. C. Kara, and M. Alizadeh, "Optimal planning of workplace electric vehicle charging infrastructure with smart charging opportunities," in *2018 21st International Conference on Intelligent Transportation Systems (ITSC)*. IEEE, 2018, pp. 1149–1154.
[8] R. S. Levinson and T. H. West, "Impact of convenient away-from-home charging infrastructure," *Transportation Research Part D: Transport and Environment*, vol. 65, pp. 288–299, 2018.
[9] Y. Zhang and L. Cai, "Dynamic charging scheduling for ev parking lots with photovoltaic power system," *IEEE Access*, vol. 6, pp. 56 995–57 005, 2018.
[10] R. Dhawan and S. Prabhakar Karthikeyan, "An efficient EV fleet management for charging at workplace using solar energy," in *2018 National Power Engineering Conference (NPEC)*, March 2018, pp. 1–5.
[11] Z. Wei, Y. Li, Y. Zhang, and L. Cai, "Intelligent parking garage EV charging scheduling considering battery charging characteristic," *IEEE Transactions on Industrial Electronics*, vol. 65, no. 3, pp. 2806–2816, March 2018.
[12] R. Jovanovic, S. Bayhan, and I. S. Bayram, "A multiobjective analysis of the potential of scheduling electrical vehicle charging for flattening the duck curve," *Journal of Computational Science*, vol. 48, p. 101262, 2021.
[13] K. Jhala, B. Natarajan, A. Pahwa, and L. Erickson, "Coordinated electric vehicle charging for commercial parking lot with renewable energy sources," *Electric Power Components and Systems*, vol. 45, no. 3, pp. 344–353, 2017.
[14] R. Jovanovic and I. S. Bayram, "Scheduling electric vehicle charging at park-and-ride facilities to flatten duck curves," in *2019 IEEE Vehicle Power and Propulsion Conference (VPPC)*. IEEE, 2019, pp. 1–5.
[15] R. Jovanovic, S. Bayhan, and I. S. Bayram, "An online model for scheduling electric vehicle charging at park-and-ride facilities for flattening solar duck curves," in *2020 International Joint Conference on Neural Networks (IJCNN)*, 2020, pp. 1–8.
[16] M. A. Ortega-Vazquez, "Optimal scheduling of electric vehicle charging and vehicle-to-grid services at household level including battery degradation and price uncertainty," *IET Generation, Transmission & Distribution*, vol. 8, no. 6, pp. 1007–1016, 2014.
[17] K. Ginigeme and Z. Wang, "Distributed optimal vehicle-to-grid approaches with consideration of battery degradation cost under real-time pricing," *IEEE Access*, vol. 8, pp. 5225–5235, 2020.
[18] Y. Shi, B. Xu, Y. Tan, and B. Zhang, "A convex cycle-based degradation model for battery energy storage planning and operation," in *2018 Annual American Control Conference (ACC)*, 2018, pp. 4590–4596.
[19] Y. Shi, B. Xu, Y. Tan, D. Kirschen, and B. Zhang, "Optimal battery control under cycle aging mechanisms in pay for performance settings," *IEEE Transactions on Automatic Control*, vol. 64, no. 6, pp. 2324–2339, 2019.
[20] Z. Wei, Y. Li, and L. Cai, "Electric vehicle charging scheme for a park-and-charge system considering battery degradation costs," *IEEE Transactions on Intelligent Vehicles*, vol. 3, no. 3, pp. 361–373, 2018.
[21] Q. Yang, J. Li, W. Cao, S. Li, J. Lin, D. Huo, and H. He, "An improved vehicle to the grid method with battery longevity management in a microgrid application," *Energy*, vol. 198, p. 117374, 2020.
[22] H. Farzin, M. Fotuhi-Firuzabad, and M. Moeini-Aghtaie, "A practical scheme to involve degradation cost of lithium-ion batteries in vehicle-to-grid applications," *IEEE Transactions on Sustainable Energy*, vol. 7, no. 4, pp. 1730–1738, 2016.
[23] K. Mainka, M. Thoben, and O. Schilling, "Lifetime calculation for power modules, application and theory of models and counting methods," in *Proceedings of the 2011 14th European Conference on Power Electronics and Applications*. IEEE, 2011, pp. 1–8.
[24] Z. J. Lee, T. Li, and S. H. Low, "ACN-data: Analysis and applications of an open EV charging dataset," in *Proceedings of the Tenth ACM International Conference on Future Energy Systems*, 2019, pp. 139–149.
[25] L. K Cherrington, J. Brooks, J. Cardenas, Z. Elgart, L. David Galicia, T. Hansen, K. Miller, M. J. Walk, P. Ryus, C. Semler, and K. Coffel, "Decision-making toolbox to plan and manage park-and-ride facilities for public transportation: Guidebook on planning and managing park-and-ride," Tech. Rep., 01 2017.
[26] J. Neff, "A profile of public transportation passenger demographics and travel characteristics reported in on-board surveys," *American Public Transportation Association and others*, 2007.
[27] InsideEVs. (2019) Monthly plug-in ev sales scorecard. [Online]. Available: https://insideevs.com/monthly-plug-in-sales-scorecard/
[28] Wikipedia. (2022) Electric vehicle battery. Accessed 2022-03-04. [Online]. Available: https://en.wikipedia.org
[29] California ISO. (2022) California ISO. [Online]. Available: http://www.caiso.com
[30] G. Mavrotas, "Effective implementation of the ε-constraint method in multi-objective mathematical programming problems," *Applied Mathematics and Computation*, vol. 213, no. 2, pp. 455 – 465, 2009.